

# Rotating MHD Convective Heat and Mass Transfer Flow of a Viscoelastic Fluid through Porous Medium in a Vertical Channel with Thermal Radiation and Soret Effect

B. P. Garg

*Research Supervisor, Punjab Technical University, Jalandhar-144002, India*

Neeraj

*Research Scholar, Punjab Technical University, Jalandhar, Punjab, India*

Ashwani Kumar Bansal

*Research Scholar, Punjab Technical University, Jalandhar, Punjab, India.*

**Abstract-** In the present paper the flow of a viscoelastic, incompressible and electrically conducting fluid in an infinite vertical channel filled with porous medium is investigated. The vertical channel and the fluid rotate in unison with a constant angular velocity  $\Omega^*$  about the axis perpendicular to the planes of the plates. A magnetic field of uniform strength is applied along the axis of rotation. The magnetic Reynolds number is assumed very small so that the induced magnetic field is neglected. A closed form solution of the governing equations is obtained for the velocity and the temperature fields. The effects of different parameters involved in the expressions for the velocity, temperature and concentration profiles are studied with the help of figures. The amplitudes and the phase angles of the wall shear stress, Nusselt number and Sherwood number are also discussed with the help of graphs.

**Keywords -** Viscoelastic, MHD convection, rotation, porous medium, radiation, Soret.

## I. INTRODUCTION

The study of MHD (magnetohydrodynamic) flow in a rotating frame of reference has important applications in design of magneto hydrodynamics power generators, aerodynamic heating, polymer technology, petroleum industry, purification of crude oil, nuclear power reactors and soil sciences. Magneto hydrodynamics (MHD) is currently undergoing through a period of tremendous developments. The interests in these new problems generate from their importance in liquid metals, electrolytes and ionized gases. On account of their varied importance, these flows have been studied by several authors e.g. Crammer and Pai [1], Ferraro and Plumpton [2], Shercliff [3].

From technological point of view, MHD free convection flows have significant applications in the field of stellar and planetary magnetosphere, aeronautics, electronics and chemical engineering on account of their varied importance. The steady and unsteady hydro magnetic rotating flows of viscous incompressible electrically conducting fluids in rotating system has drawn attention of a number of scholars e.g. Seth and Jana [4], Seth et al [5], Guria et al. [6] etc.. During the last few decades the applications of rotating flow finds its application in engineering disciplines also, such as in the food processing industry, chemical process industry, centrifugation and filtration processes and rotating machinery. In recent years a number of studies have also appeared in the literature on the fluid phenomena on earth involving rotation to a greater or lesser extent viz. Vidyanidhu and Nigam [7], Gupta [8], Jana and Datta [9]. Mazumder [10] obtained an exact solution of an oscillatory Couette flow in a rotating system. Thereafter Ganapathy [11] presented the solution for rotating Couette flow. Singh [12] analyzed the oscillatory magneto hydrodynamic (MHD) Couette flow in a rotating system in the presence of transverse magnetic

field. Singh [13] also obtained an exact solution of magneto hydrodynamic (MHD) mixed convection flow in a rotating vertical channel with heat radiation. An unsteady hydro magnetic free convection flow with radiative heat transfer in a rotating fluid flow is analyzed by Bestman and Adiepong [14]. Seth et al. [15] studied an unsteady convective flow within a parallel plate rotating channel with thermal source/sink in a porous medium under slip condition. Chandran et al. [16] studied the rotational effect on unsteady hydro magnetic Couette flow. Transient effect on magneto hydrodynamic Couette flow with rotation is investigated by Singh et al. [17]. Prasad Rao et al. [18] studied combined effect of free and forced convection on MHD flow in a rotating porous channel. Soundalgekar and Pop [19] analyzed hydro magnetic flow in a rotating fluid past an infinite porous plate. Singh and Mathew [20] studied the effects of injection/suction on an oscillatory hydro magnetic flow in a rotating horizontal porous channel.

At the high temperature attained in some engineering devices, for example, gas can be ionized and so becomes an electrical conductor. The ionized gas or plasma can be made to interact with the magnetic field and alter heat transfer and friction characteristic. Recently, it is of great interest to study the effect of magnetic field on the convective flows when the fluid is not only an electrical conductor but also when it is capable of emitting and absorbing thermal radiation. The heat transfer by thermal radiation is becoming of greater importance when we are concerned with space applications, higher operating temperatures and also power engineering. The radiative free convective flows are encountered in countless industrial and environment processes e.g. heating and cooling chambers, fossil fuel combustion energy processes, evaporation from large open water reservoirs, astrophysical flows, and solar power technology and space vehicle re-entry. The radiative heat transfer plays an important role in manufacturing industries for the design of reliable equipment. Nuclear power plants, gas turbines and various propulsion devices for aircraft, missiles, satellites and space vehicles are examples of such engineering applications. Alagoa et al. [21] analyzed the effects of radiation on free convection MHD flow through porous medium between infinite parallel plates in the presence of time-dependent suction. Mebine [22] studied the radiation effects on MHD Couette flow with heat transfer between two parallel plates. Singh and Kumar [23] obtained an exact solution of free convective oscillatory flow through porous medium in a rotating vertical channel. Singh and Garg [24] have also obtained exact solution of an oscillatory free convection MHD flow in a rotating channel in the presence of heat transfer due to radiation. Recently Garg [25] studied combined effects of thermal radiations and Hall current on moving vertical porous plate in a rotating system with variable temperature. Very recently, assuming the temperature of one of the plate varying with time, Singh [26] analyzed an oscillatory MHD convective flow of a viscoelastic fluid through a porous medium in a rotating vertical channel in slip-flow regime with thermal radiation and Hall current.

On the other hand, simultaneous heat and mass transfer from different geometries embedded in porous media has many engineering and geophysical applications such as drying of porous solids, thermal insulations, cooling of nuclear reactors and underground energy transport. Singh and Kumar [27] analyzed fluctuating heat and mass transfer on unsteady MHD free convection flow of radiating and reacting fluid past a vertical porous plate in slip-flow regime. Kumar and Singh [28] studied sores and Hall effects on oscillatory MHD free convective flow of radiating fluid in a rotating vertical porous channel filled with porous medium. Singh et al. [29] analyzed heat and mass transfer in an unsteady MHD free convective flow through a porous medium bounded by vertical porous channel in the presence of radiative heat and Hall current. Recently, Garg [30] investigated magnetohydrodynamics and radiation effects on the flow due to moving vertical porous plate with variable temperature. The aim of this study is to analyze the MHD convection flow through porous medium in a rotating vertical channel in the presence of molecular and thermal diffusions. The heat radiation effect is also taken into account for this heat transfer problem. A uniform magnetic field is applied transverse to the flow. The fluid and the channel rotate as a solid body about an axis normal to the planes of the channel plates. An exact solution of the flow problem is obtained and the effects of different flow parameters on the results are discussed with the help of graphs.

## II. BASIC EQUATIONS

In order to derive basic equations for the problem under consideration following assumptions are made:

- (i) The flow considered is unsteady and laminar between two infinite electrically non-conducting vertical plates.
- (ii) The fluid is finitely conducting and with constant physical properties.
- (iii) A magnetic field of uniform strength is applied normal to the flow.
- (iv) The magnetic Reynolds number is taken small enough so that the induced magnetic field is neglected.
- (v) Hall effect, electrical and polarization effects are neglected.
- (vi) It is assumed that the fluid is optically-thin gray gas, absorbing/ emitting radiation and non-scattering.
- (vii) The entire system (consisting of channel plates and the fluid) rotates about an axis perpendicular to the planes of the plates.
- (viii) Since plates are infinite so all physical quantities except pressure depend only on  $z^*$  and  $t^*$ .

Under these assumptions, we write hydro magnetic equations of continuity, motion, energy and concentration in a rotating frame of reference as:

$$\nabla \cdot \mathbf{V} = 0, \quad (1)$$

$$\frac{\partial \mathbf{V}}{\partial t} + (\mathbf{V} \cdot \nabla) \mathbf{V} + 2\boldsymbol{\Omega} \times \mathbf{V} = \nabla \cdot \boldsymbol{\Xi} - \frac{\rho_1}{K} \mathbf{V} + \frac{1}{\rho} (\mathbf{J} \times \mathbf{B}) + \mathbf{F}, \quad (2)$$

$$\frac{\partial T^*}{\partial t^*} + (\mathbf{V} \cdot \nabla) T^* = \frac{k}{\rho c_p} \nabla^2 T^* - \frac{q_0}{\rho c_p}, \quad (3)$$

$$\frac{\partial C^*}{\partial t^*} + (\mathbf{V} \cdot \nabla) C^* = D \nabla^2 C^* + D_T \nabla^2 T^* - K_T (C^* - C_1). \quad (4)$$

In equation (2) the last term on the left hand side is the Coriolis force. On the right hand side of (2) the last term  $\mathbf{F} = g\beta(T^* - T_1) + g\beta^*(C^* - C_1)$  accounts for the force due to buoyancy and the second last term is the Lorentz force due to magnetic field  $\mathbf{B}$  and is given by

$$\mathbf{J} \times \mathbf{B} = \sigma(\mathbf{V} \times \mathbf{B}) \times \mathbf{B}. \quad (5)$$

In the first term on the R. H. S. of equation (2),  $\boldsymbol{\Xi}$  are the Cauchy stress tensor and the constitutive equation derived by Coleman and Noll [31] for an incompressible homogeneous fluid of second order is

$$\boldsymbol{\Xi} = -p^* \mathbf{I} + \mu_1 \mathbf{A}_1 + \mu_2 \mathbf{A}_2 + \mu_3 \mathbf{A}_1^2. \quad (6)$$

Here  $-p^* \mathbf{I}$  is the interdeterminate part of the stress due to constraint of incompressibility,  $\mu_1$ ,  $\mu_2$  and  $\mu_3$  are the material constants describing viscosity, elasticity and cross-viscosity respectively. The kinematic  $\mathbf{A}_1$  and  $\mathbf{A}_2$  are the Rivelen Ericson constants defined as

$$\mathbf{A}_1 = (\nabla \mathbf{V}) + (\nabla \mathbf{V})^T, \quad \mathbf{A}_2 = \frac{d\mathbf{A}_1}{dt} + (\nabla \mathbf{V})^T \mathbf{A}_1 + \mathbf{A}_1 (\nabla \mathbf{V}),$$

where  $\nabla$  denotes the gradient operator and  $d/dt$  the material time derivative. According to Markovitz and Coleman [32] the material constants  $\mu_1$ ,  $\mu_2$  are taken as positive and  $\mu_3$  as negative. The modified pressure  $p^* = p' - \frac{\rho}{2} |\boldsymbol{\Omega} \times \mathbf{R}|^2$ , where  $\mathbf{R}$  denotes the position vector from the axis of rotation,  $p'$  denotes the fluid pressure,  $\mathbf{J}$  is the current density and all other quantities have their usual meanings and have been defined in the text time to time.

The last term in equation (3) stands for heat due to radiation and is given by

$$\frac{\partial q_0}{\partial z^*} = 4\alpha^* \sigma^* (T^{*4} - T_1^4), \quad (7)$$

for an optically thin gray gas. Here  $\alpha^*$  is the mean absorption coefficient and  $\sigma^*$  is Stefan- Boltzmann constant. We assume that the temperature differences within the flow are sufficiently small such that  $T^{*4}$  may be expressed as a linear function of the temperature. This is accomplished by expanding  $T^{*4}$  in a Taylor series about  $T_1$  and neglecting higher order terms, thus

$$T^{*4} \approx 4T_1^3 T^* - 3T_1^4. \tag{8}$$

Substituting (8) into (7) and simplifying, we obtain

$$\frac{\partial \theta^*}{\partial z^*} = 16\alpha^* \sigma^* T_1^3 (T^* - T_1). \tag{9}$$

The substitution of equation (9) into the energy equation (3) for the heat due to radiation, we get

$$\frac{\partial T^*}{\partial t^*} + (\mathbf{V} \cdot \nabla) T^* = \frac{k}{\rho c_p} \nabla^2 T^* - \frac{16\alpha^* \sigma^* T_1^3}{\rho c_p} (T^* - T_1). \tag{10}$$

### III. FORMULATION OF THE PROBLEM

We consider an unsteady flow of a viscoelastic (second order) incompressible and electrically conducting fluid bounded by two infinite insulated vertical plates distance ‘d’ apart as shown in Fig.1. A coordinate system is chosen such that the  $X^*$  -axis is oriented upward along the centerline of the channel and  $Z^*$ -axis taken perpendicular to the planes of the plates lying in  $xy^*$  planes. The non-uniform temperature of the plate at  $z^* = \pm \frac{d}{2}$  and the species concentration at the plate  $z^* = -\frac{d}{2}$  are respectively assumed to be varying periodically with time. The  $Z^*$  - axis is considered to be the axis of rotation about which the fluid and the plates are assumed to be rotating as a solid body with a constant angular velocity  $\Omega$  (0, 0,  $\Omega^*$ ). A transverse magnetic field of uniform strength  $\mathbf{B}$  (0, 0,  $B_0$ ) is also applied along the axis of rotation. For impermeable plates of the channel, the velocity may reasonably be assumed with its components along  $x^*$ ,  $y^*$ ,  $z^*$  directions as  $\mathbf{V}$  ( $u^*$ ,  $v^*$ , 0). Since the plates are infinite in  $X^*$ -direction so all physical quantities except pressure depend only on  $z^*$  and  $t^*$ . The equation of continuity (1) is then satisfied identically for non-porous plates. A schematic diagram of the physical problem considered is shown in Figure 1.

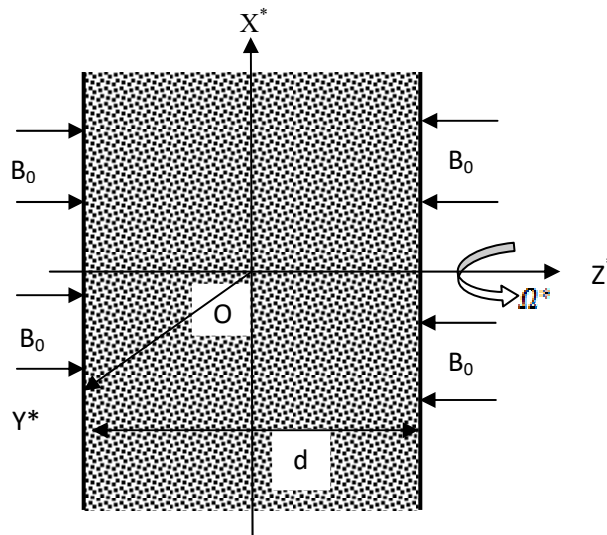


Fig.1. Physical configuration of the physical problem.

Using the velocity and the magnetic field distribution as stated above the magneto hydrodynamic (MHD) flow in the rotating channel is governed by the following Cartesian equations:

$$\frac{\partial u^*}{\partial t^*} - 2\Omega^* v^* = -\frac{1}{\rho} \frac{\partial p^*}{\partial x^*} + \vartheta_1 \frac{\partial^2 u^*}{\partial z^{*2}} + \vartheta_2 \frac{\partial^2 u^*}{\partial z^{*2} \partial t^*} - \frac{\sigma B_0^2}{\rho} u^* - \frac{\partial_1 u^*}{N^*} + g\beta(T^* - T_1) + g\beta^*(C^* - C_1), \quad (11)$$

$$\frac{\partial v^*}{\partial t^*} + 2\Omega^* u^* = -\frac{1}{\rho} \frac{\partial p^*}{\partial y^*} + \vartheta_1 \frac{\partial^2 v^*}{\partial z^{*2}} + \vartheta_2 \frac{\partial^2 v^*}{\partial z^{*2} \partial t^*} - \frac{\sigma B_0^2}{\rho} v^* - \frac{\partial_1 v^*}{N^*}, \quad (12)$$

$$0 = -\frac{1}{\rho} \frac{\partial p^*}{\partial z^*}, \quad (13)$$

$$\frac{\partial T^*}{\partial t^*} = \frac{k}{\rho c_p} \frac{\partial^2 T^*}{\partial z^{*2}} - \frac{16\sigma^* \epsilon^* T_1^3}{\rho c_p} (T^* - T_1), \quad (14)$$

$$\frac{\partial C^*}{\partial t^*} = D \frac{\partial^2 C^*}{\partial z^{*2}} + D_T \frac{\partial^2 T^*}{\partial z^{*2}} - K_r (C^* - C_1), \quad (15)$$

where  $\rho$  is the density,  $\vartheta_1$  is the kinematic viscosity,  $\vartheta_2$  is the viscoelasticity,  $p^*$  is the modified pressure,  $t^*$  is the time,  $\sigma$  is the electric conductivity,  $g$  is the acceleration due to gravity,  $\beta$  is the volumetric coefficient of thermal expansion,  $\beta^*$  is the volumetric coefficient of expansion with concentration,  $k$  is the thermal conductivity,  $c_p$  is the specific heat at constant pressure,  $D$  is the molecular diffusivity,  $D_T$  is the coefficient of thermal diffusion and  $K_r$  is the chemical reaction. Equation (13) shows the constancy of the hydrodynamic pressure along the axis of rotation.

The boundary conditions for the problem are

$$z^* = -\frac{d}{2} \quad u^* = v^* = 0, T^* = T_1, C^* = C_1 + (C_2 - C_1) \cos \omega^* t^*, \quad (16)$$

$$z^* = \frac{d}{2} \quad u^* = v^* = 0, T^* = T_1 + (T_2 - T_1) \cos \omega^* t^*, C^* = C_1, \quad (17)$$

where  $\omega^*$  is the frequency of oscillations.

Introducing the following non-dimensional quantities into equations (11) and (15)

$$x = \frac{u^*}{U}, y = \frac{v^*}{U}, z = \frac{z^*}{d}, t = \frac{t^* U}{d}, \omega = \frac{\omega^* d}{U}, u = \frac{u^*}{U}, v = \frac{v^*}{U}, \theta = \frac{T^* - T_1}{T_2 - T_1}, C = \frac{C^* - C_1}{C_2 - C_1}, p = \frac{p^*}{\rho U^2}, \quad (18)$$

we get

$$Re \frac{\partial u}{\partial t} - 2\Omega v = -Re \frac{\partial p}{\partial x} + \frac{\partial^2 u}{\partial z^2} + \gamma Re \frac{\partial^2 u}{\partial z^2 \partial t} - (M^2 + K^{-1})u + Gr \theta + Grm C, \quad (19)$$

$$Re \frac{\partial v}{\partial t} + 2\Omega u = -Re \frac{\partial p}{\partial y} + \frac{\partial^2 v}{\partial z^2} + \gamma Re \frac{\partial^2 v}{\partial z^2 \partial t} - (M^2 + K^{-1})v, \quad (20)$$

$$RePr \frac{\partial \theta}{\partial t} = \frac{\partial^2 \theta}{\partial z^2} - N^2 \theta, \quad (21)$$

$$ReSc \frac{\partial C}{\partial t} = \frac{\partial^2 C}{\partial z^2} + S_0 S_1 \frac{\partial^2 \theta}{\partial z^2} - K_r S_0 C, \quad (22)$$

where  $U$  is the mean axial velocity, ‘\*’ represents the dimensional quantities,

$$\Omega = \frac{\Omega^* d^2}{U} \text{ is the rotation parameter,}$$

$\gamma = \frac{\mu_0}{\rho_0 \nu}$  is the visco-elastic parameter,

$Re = \frac{U d}{\nu_1}$  is the Reynolds number,

$Gr = \frac{g \beta d^3 (\bar{T}_1 - \bar{T}_2)}{\nu_1 U}$  is the Grashof number,

$Gm = \frac{g \beta d^3 (\theta_1 - \theta_2)}{\nu_1 U}$  is the modified Grashof number,

$M = B_0 d \sqrt{\frac{\sigma}{\rho \nu_1}}$  is the Hartmann number,

$K = \frac{\mu_0^2}{\rho_0 \nu}$  is the permeability of the porous medium,

$Pr = \frac{\rho \nu_1 c_p}{k}$  is the Prandtl number,

$N = 4d \sqrt{\frac{\sigma \epsilon^* T_f^3}{k}}$  is the radiation parameter,

$Sc = \frac{\nu_1}{D}$  is the Schmidt number,

$S_0 = \frac{D_0 (\bar{T}_1 - \bar{T}_2)}{\nu_1 (\theta_1 - \theta_2)}$  is the sores parameter,

$K_r = \frac{R_0 d^2}{\nu_1}$  is the chemical reaction parameter.

The boundary conditions in the dimensionless form become

$$z = -\frac{1}{2} \quad u = v = 0, \quad \theta = 0, \quad C = \cos \omega t, \quad (23)$$

$$z = \frac{1}{2} \quad u = v = 0, \quad \theta = \cos \omega t, \quad C = 0. \quad (24)$$

We shall assume now that the fluid flows under the influence of pressure gradient varying periodically with time in the  $X^*$ -axis only is of the form

$$-\frac{\partial p}{\partial x} = A \cos \omega t \quad \text{and} \quad -\frac{\partial p}{\partial y} = 0, \quad (25)$$

where A is a constant.

#### IV. SOLUTION OF THE PROBLEM

Now combine equations (19) and (20) into single equation by introducing a complex function  $F = u + iv$ , we get

$$Re \frac{\partial F}{\partial t} + 2i\Omega F = A \cos \omega t + \frac{\partial^2 F}{\partial z^2} + \gamma Re \frac{\partial^2 F}{\partial z^2 \partial t} - (M^2 + K^{-1})F + Gr \theta + Gm C. \quad (26)$$

In order to solve the problem it is convenient to adopt complex notations and assume the solution of the problem as

$$F(z, t) = F_0(z) e^{i\omega t}, \quad \theta(z, t) = \theta_0(z) e^{i\omega t}, \quad C(z, t) = C_0(z) e^{i\omega t}, \quad -\frac{\partial p}{\partial x} = A \cos \omega t = A e^{i\omega t}, \quad (27)$$

with corresponding boundary conditions as

$$z = -\frac{1}{2} \quad F = 0, \quad \theta = 0, \quad C = \cos \omega t, \tag{28}$$

$$z = \frac{1}{2} \quad F = 0, \quad \theta = \cos \omega t, \quad C = 0. \tag{29}$$

The boundary conditions (28) and (29) in complex notations can also be written as

$$z = -\frac{1}{2} \quad F = 0, \quad \theta = 0, \quad C = e^{i\omega t}, \tag{30}$$

$$z = \frac{1}{2} \quad F = 0, \quad \theta = e^{i\omega t}, \quad C = 0. \tag{31}$$

Substituting expressions (27) in equations (26), (21) and (22), we get

$$\alpha^2 \frac{d^2 F_0}{dz^2} - m^2 F_0 = -AR\alpha - Gr\theta_0 - GmC_0, \tag{32}$$

$$\frac{d^2 \theta_0}{dz^2} - n^2 \theta_0 = 0, \tag{33}$$

$$\frac{d^2 C_0}{dz^2} - l^2 C_0 = -\gamma_x \gamma_0 \frac{d^2 \theta_0}{dz^2}, \tag{34}$$

where  $\alpha = \sqrt{1 + \omega \mu R \rho}$ ,  $l = \sqrt{Sc(K_r + \omega R \rho)}$ ,  $m = \sqrt{N^2 + K^{-1} + 2i\Omega + \omega R \rho}$ ,  $n = \sqrt{N^2 + \omega R \rho Pr}$ .

The transformed boundary conditions reduce to

$$z = -\frac{1}{2} \quad F_0 = 0, \quad \theta_0 = 0, \quad C_0 = 1, \tag{35}$$

$$z = \frac{1}{2} \quad F_0 = 0, \quad \theta_0 = 1, \quad C_0 = 0. \tag{36}$$

The ordinary differential equations (32), (33) and (34) are solved under the boundary conditions (35) and (36) for the velocity, temperature and species concentration fields. The solution of the problem is obtained as

$$F(z, t) = \left[ \begin{aligned} & \frac{AR\alpha}{m^2} \left( 1 - \frac{\cosh \frac{mz}{\alpha}}{\cosh \frac{m}{\alpha}} \right) + \frac{Gr}{(\alpha^2 n^2 - m^2)} \left( \frac{\sinh \frac{m}{\alpha} (\frac{1}{2} - z)}{\sinh \frac{m}{\alpha}} - \frac{\sinh n (\frac{1}{2} - z)}{\sinh n} \right) \\ & + \frac{Gm}{(\alpha^2 l^2 - m^2)} \left( \frac{\sinh \frac{m}{\alpha} (\frac{1}{2} - z)}{\sinh \frac{m}{\alpha}} - \frac{\sinh l (\frac{1}{2} - z)}{\sinh l} \right) \\ & - \frac{G\gamma_x \gamma_0 \alpha^2}{(n^2 - l^2)} \left( \frac{\sinh l (\frac{1}{2} - z)}{(\alpha^2 l^2 - m^2) \sinh l} - \frac{\sinh n (\frac{1}{2} - z)}{(\alpha^2 n^2 - m^2) \sinh n} - \frac{\alpha^2 (n^2 - l^2) \sinh \frac{m}{\alpha} (\frac{1}{2} - z)}{(\alpha^2 l^2 - m^2)(\alpha^2 n^2 - m^2) \sinh \frac{m}{\alpha}} \right) \end{aligned} \right] e^{i\omega t}. \tag{37}$$

$$\theta(z, t) = \frac{\sinh n (\frac{1}{2} - z)}{\sinh n} e^{i\omega t}, \tag{38}$$

$$C(z, t) = \left[ \frac{\sinh l (\frac{1}{2} - z)}{\sinh l} + \frac{\gamma_x \gamma_0 \alpha^2}{(n^2 - l^2)} \left( \frac{\sinh l (\frac{1}{2} - z)}{\sinh l} - \frac{\sinh n (\frac{1}{2} - z)}{\sinh n} \right) \right] e^{i\omega t}. \tag{39}$$

The primary velocity is given by the real part of complex function F (z,t).

From the velocity field we can now obtain the skin-friction  $\tau_w$  at the left plate in terms of its amplitude and phase angle as

$$\tau_w = \left( \frac{\partial F}{\partial z} \right)_{z = -\frac{1}{2}} = |F| \cos(\omega t + \phi), \tag{40}$$

$$\text{with } H_p + i H_f = \frac{Gr \gamma}{ma} \tanh \frac{M}{2a} + \frac{Gr}{(a^2 n^2 - m^2)} \left( \frac{M}{\sinh \frac{M}{2}} - \frac{n}{\sinh n} \right) - \frac{Gr}{(a^2 \beta - m^2)} \left( \frac{M}{2} \coth \frac{M}{2} - l \coth l \right) - \frac{Gr S_0 S_0 n^2}{(a^2 \beta - \beta^2)} \left\{ \frac{l}{(a^2 \beta - m^2) \sinh l} - \frac{n}{(a^2 n^2 - m^2) \sinh n} - \frac{am(n^2 - \beta)}{(a^2 \beta - m^2)(a^2 n^2 - m^2) \sinh \frac{M}{2}} \right\}. \quad (41)$$

$$\text{The amplitude is } |H| = \sqrt{H_p^2 + H_f^2} \text{ and the phase angle } \varphi = \tan^{-1} \frac{H_f}{H_p}. \quad (42)$$

From the temperature field given in equation (38) the heat transfer coefficient Nu (Nusselt number) in terms of its amplitude and the phase angle can be obtained as

$$Nu = \left( \frac{\partial T}{\partial z} \right)_{z=-\frac{1}{2}} = |H| \cos(\omega t + \varphi), \quad (43)$$

$$\text{where } H_p + i H_f = \frac{n}{\sinh n}. \quad (44)$$

The amplitude  $|H|$  and the phase angle  $\varphi$  of the heat transfer coefficient Nu (Nusselt number) are given by

$$|H| = \sqrt{H_p^2 + H_f^2} \text{ and } \varphi = \tan^{-1} \left( \frac{H_f}{H_p} \right) \text{ respectively.} \quad (45)$$

Similarly, The amplitude and the phase angle of the Sherwood number at the left plate ( $z=-0.5$ ) can be obtained from equation (39) for the species concentration as

$$Sh = \left( \frac{\partial C}{\partial z} \right)_{z=-\frac{1}{2}} = |C| \cos(\omega t + \zeta), \quad (46)$$

$$\text{where } C_p + i C_f = -l \coth l + \frac{Gr S_0 n^2}{(a^2 \beta - \beta^2)} \left( \frac{l}{\sinh l} - \frac{n}{\sinh n} \right). \quad (47)$$

The amplitude  $|C|$  and the phase angle  $\zeta$  of Sherwood number (Sh) are given by

$$|C| = \sqrt{C_p^2 + C_f^2} \text{ and } \zeta = \tan^{-1} \left( \frac{C_f}{C_p} \right) \text{ respectively.} \quad (48)$$

## V. DISCUSSION OF THE RESULTS

The problem of unsteady magnetohydrodynamic (MHD) convective and radiative flow in a vertical porous channel is analyzed when the temperature and the species concentration of the plates vary periodically with time. The entire system (consisting of channel plates and the fluid) rotates about an axis perpendicular to the plates. The closed form solutions for the velocity and temperature fields are obtained analytically and then evaluated numerically for different values of parameters appeared in the equations. In this study, air is considered to be a primary fluid (solvent) and to produce a significant effect on mass diffusion, some fluids, considered as secondary (solute) such as Hydrogen (H<sub>2</sub>), Water vapor (H<sub>2</sub>O), Ammonia (NH<sub>3</sub>), and carbon-dioxide (CO<sub>2</sub>) have been diffused through air. Throughout the discussion, the values of Schmidt number (Sc) of the corresponding secondary species are taken as 0.22, 0.60, 0.78, 0.94 and the Prandtl number (Pr) of the diffused fluids are taken as 0.7 and 7.0, representing air and water at one atmosphere of pressure. To have better insight of the physical problem the variations of the velocity, temperature, skin-friction rate of heat transfer in terms of their amplitudes and phase angles are evaluated numerically for different sets of the values for small and large rotation parameter  $\Omega$ , visco-elastic parameter  $\gamma$ , Reynolds number Re, Grashof number Gr, modified Grashof number Gm, Hartmann number M, permeability of the porous medium K, Prandtl number Pr, radiation parameter N, pressure gradient A, Schmidt number S<sub>c</sub>, Soret number S<sub>o</sub>, reaction parameter K<sub>r</sub> and the frequency of oscillations  $\omega$ . In each figure the smooth and the dotted (---) curves show variations for small ( $\Omega=10$ ) and large ( $\Omega=20$ ) rotations respectively.

Fig.2 illustrates the variation of the velocity with the increasing rotation of the system. It is quite obvious from this figure that velocity goes on decreasing with increasing rotation  $\Omega$  of the entire system. The velocity profiles initially remain parabolic with maximum at the centre of the channel for small values of rotation parameter  $\Omega=5$  and then as rotation increases i.e.,  $\Omega=10$ , the velocity profiles flatten. For further increase in rotation ( $\Omega= 20, 30$ ) the maximum of velocity profiles no longer occurs at the centre but shift towards the walls of the channel. It means that for large rotation there arise boundary layers on the walls of the channel. The effect of the viscoelastic parameter  $\gamma$  on the velocity profiles are shown in Fig. 3. The figure clearly shows that the velocity decreases tremendously with the increasing values of  $\gamma$  for the small ( $\Omega = 10$ ) and large ( $\Omega= 20$ ) rotation of the system. For given values of other parameters the velocity is maximum in the case of Newtonian fluid i.e.,  $\gamma=0$ . Figure 4 depicts that the velocity increases with increasing Reynolds number  $Re$  for small and large rotations both.

The variations of the velocity profiles with the Grashof number  $Gr$  are presented in Fig.5. For small ( $\Omega=10$ ) and large ( $\Omega=20$ ) rotations, the velocity increases with increasing Grashof number. The maximum of the parabolic velocity profiles shifts toward right half of the channel due to the greater buoyancy force in this part of the channel due to the presence of hotter plate. Similarly, the effects of modified Grashof number  $G_m$  are presented in Figure 6 and it is observed that the velocity increases with increasing  $G_m$  for both the cases of small ( $\Omega=10$ ) and large ( $\Omega=20$ ) rotations of the channel. In this case the maximum of the parabolic velocity profiles shifts toward left half of the channel due to the higher species concentration in that part of the channel.

The effects of the magnetic field on the velocity field are illustrated in Fig.7. It is observed that with increasing Hartmann number  $M$  velocity decreases for small ( $\Omega=10$ ) rotation but increases for large ( $\Omega=20$ ) rotations. This means that increasing Lorentz force due to increasing magnetic field strength resists the backward flow caused by the large rotation of the system. Fig.8 shows the variations of the velocity with the permeability of the porous medium  $K$ . It is observed from the figure that the velocity decrease with the increase of  $K$  for both small ( $\Omega=10$ ) and large ( $\Omega=20$ ) rotations of the system. This means that the resistance posed by the porous matrix to the retarding flow due to rotation of the channel reduces with increasing permeability. We find from Fig.9 that with the increase of Prandtl number  $Pr$  the velocity decreases for small ( $\Omega=10$ ) and large ( $\Omega=20$ ) rotations both. Fig.10 shows that for small ( $\Omega=10$ ) and large ( $\Omega=20$ ) rotations both the velocity decreases with increasing radiation parameter  $N$ . It is observed from Figs.11 that the effect of Schmidt number  $Sc$  on velocity is insignificant. However, the velocity decreases with the increase of chemical reaction parameter  $K_r$  but increases with increasing sorlet parameter  $S_o$  for small ( $\Omega=10$ ) and large ( $\Omega=20$ ) rotations both as is clear from Figures 12 and 13. The effect of the frequency of oscillations  $\omega$  on the velocity is exhibited in Fig.14. It is noticed that velocity decreases with increasing frequency  $\omega$  for either case of channel rotation large or small.

The temperature profiles are shown in Figure 15. It is quite clear from this figure that the temperature decreases with the increase of each of the parameters involved i.e., Reynolds number, Prandtl number  $Pr$ , radiation parameter  $N$  and the frequency of oscillations  $\omega$ . Similarly, Fig.16 shows that the species concentration increases with the increase of Reynolds number  $Re$ , sorlet parameter  $S_o$  and the frequency of oscillations  $\omega$  but decreases with chemical reaction parameter  $K_r$ . The variation in species concentration is insignificant due to the increase of Schmidt number  $Sc$ . A careful study of the curves reveals that the species decreases in left half but increases in right half of the channel. The amplitude  $|N|$  and the phase angle of the Nusselt number are presented in Figures 17 and 18 respectively. Figure 17 reveals that  $|N|$  decreases sharply with the increase of Reynolds number and the Prandtl number as frequency  $\omega$  increases. However, the amplitude remains almost constant for increased radiation parameter  $N$  as  $\omega$  increases. The amplitude remains almost constant with increasing frequency of oscillations  $\omega$ . The phase angle  $\psi$  of rate of heat transfer shown in figure 18 oscillates between phase lag and phase lead for increased Reynolds number  $Re$  and the Prandtl number  $Pr$  as frequency of oscillations  $\omega$  increases. Over the values of  $\omega$  chosen a phase lag is noticed for small Reynolds number and increased radiation parameter  $N$ . The amplitude  $|C|$  and phase angle  $\zeta$  of the Sherwood number are shown in Figures 19 and 20. Figure 19 shows that the amplitude  $|C|$  increases with the increase of Reynolds number  $Re$ , Schmidt number  $Sc$  and reaction parameter  $K_r$  but decreases

with the increase of sorlet number  $S_o$ . It is also very clear from figure 20 that the phase angle  $\zeta$  increases with the increase of Reynolds number  $Re$  and Schmidt number  $Sc$  but decreases with the increase of reaction parameter  $K_r$ . A phase lead is observed for increased  $Re$ ,  $S_c$  and  $K_r$  but for increased sorlet number  $S_o$  there is a phase lag.

The skin-friction  $\tau_z$  in terms of its amplitude  $|F|$  and phase angle  $\varphi$  has been shown in Figures. 21 and 22 respectively for the sets of values listed in Table 1. The effect of each of the parameter on  $|F|$  and  $\varphi$  is assessed by comparing each curve with dotted curves I in these figures. In Figure.21 the comparison of the curves V, VI, VIII, and XII with dotted curve I (---) indicate that the amplitude increases with the increase of Grashof number  $Gr$ , modified Grashof number  $Gm$ , permeability of the porous medium  $K$  and sorlet parameter  $S_o$ . Similarly the comparison of the curves II, III, VII, IX, X, XI and XIII with dotted curve I depicts that the skin-friction amplitude decreases with the increase of rotation parameter  $\Omega$ , viscoelastic parameter  $\gamma$ , Hartmann number  $M$ , Prandtl number  $Pr$ , radiation parameter  $N$ , Schmidt number  $S_c$  and chemical reaction  $K_r$ . It is interesting to note that with the increase of Reynolds number  $Re$  skin friction amplitude increases for small values of  $\omega$  but then decreases for large values of  $\omega$ . It is obvious that  $|F|$  goes on decreasing gradually with increasing frequency of oscillations  $\omega$ . It is clear from figure 22 showing the variations of the phase angle  $\varphi$  of the skin-friction that there is always a phase lag because the values of  $\varphi$  remain negative throughout. Comparing curves II, III, IV, V, VI, VIII and XI with dotted curve I (---) it is observed that the phase lag increases with the increase of rotation parameter  $\Omega$ , viscoelastic parameter  $\gamma$ , Reynolds number  $Re$ , Grashof number  $Gr$ , modified Grashof number  $Gm$ , permeability of the porous medium  $K$  and Schmidt number  $Sc$ . Also the comparison of curves VII, IX, X, XII and XIII with dotted curve I (---) indicate that the phase lag decreases with the increase of Hartmann number  $M$ , Prandtl number  $Pr$ , radiation parameter  $N$ , sorlet parameter  $S_o$  and the chemical reaction parameter  $K_r$ . Phase lag goes on increasing with increasing frequency of oscillations  $\omega$ .

## VI. CONCLUSIONS

An unsteady rotating MHD convective flow of viscoelastic, incompressible and electrically conducting fluid in a vertical channel is investigated. The entire system consisting of channel plates and the fluid rotates about an axis perpendicular to the plates. A closed form solution of the problem is obtained. Following features are concluded from the mathematical analysis:-

- (i) It is found that with the increasing rotation of the channel the primary velocity decreases and the maximum of the parabolic velocity profiles at the centre of the channel shifts towards the walls of the channel.
- (ii) The velocity increases with the increase of Reynolds number  $Re$ , Grashof number  $Gr$ , modified Grashof number  $Gm$  and Sorlet parameter  $S_o$ .
- (iii) But  $u(z, t)$  decreases with increasing rotation  $\Omega$ , viscoelastic parameter  $\gamma$ , permeability of porous medium  $K$ , Prandtl number  $Pr$ , radiation parameter  $N$ , reaction parameter and frequency of oscillations  $\omega$ .
- (iv) The amplitude  $|F|$  of the skin-friction increases due to the increase of Grashof number, modified Grashof number, permeability of porous medium and sorlet parameter.
- (v) Similarly, the amplitude  $|F|$  of the skin-friction decreases due to the increase of rotation parameter, viscoelastic parameter, Prandtl number, radiation parameter.
- (vi) There is always a phase lag of the shear stress.
- (vii) The temperature and the amplitude of the rate of heat transfer decrease with the increase of any of the parameters that appear.
- (viii) The phase of  $Nu$  oscillates between phase lag and phase lead for increased Reynolds number  $Re$  and the Prandtl number  $Pr$  as frequency of oscillations  $\omega$  increases.
- (ix) The amplitude of Nusselt number decreases sharply with the increase of Reynolds number and the Prandtl number as frequency  $\omega$  increases.
- (x) The amplitude of Sherwood number increases with the increase of Reynolds number  $Re$ , Schmidt number  $Sc$  and reaction parameter.

## NOMENCLATURE

$A$  – constant  
 $a^*$  – is the mean absorption coefficient  
 $B_0$  – intensity of the applied magnetic field  
 $C$  – Dimensionless species concentration of the fluid  
 $C_p$  – specific heat at constant pressure  
 $C_1$  – species concentration at the plate  
 $C_2$  – species concentration of the fluid at the plate  
 $D$  – Coefficient of chemical molecular mass diffusivity  
 $D_T$  – coefficient of chemical thermal diffusivity  
 $G_m$  – Grashof number for mass transfer  
 $G_r$  – Grashof number for heat transfer  
 $K$  – Permeability of the porous medium  
 $K_r$  – chemical reaction parameter  
 $K$  – thermal conductivity  
 $M$  – Magnetic field parameter (Hartmann number)  
 $Pr$  – Prandtl number  
 $S_c$  – Schmidt number  
 $S_o$  – Soret number  
 $T$  – temperature of the fluid  
 $T_1$  – fluid temperature at the plate  
 $T_2$  – fluid temperature at the plate  
 $t$  – Time  
 $u$  –  $x$ -component of the velocity vector  
 $U$  – Reference velocity  
 $v$  –  $y$ -component of velocity vector  
 $\beta$  – Coefficient of volume expansion for heat transfer  
 $\beta^*$  – coefficient of volume expansion for mass transfer  
 $\rho$  – fluid density in the boundary layer  
 $\nu_1$  – kinematic viscosity  
 $\nu_2$  – viscoelasticity  
 $\sigma$  – electric conductivity  
 $\sigma^*$  – is Stefan- Boltzmann constant.  
 $\theta$  – dimensionless temperature  
 $\varphi$  – phase of shear stress  
 $\psi$  – phase of Nusselt number  
 $\zeta$  – phase of Sherwood number  
 $\Omega$  – rotation parameter  
 $\omega$  – frequency of oscillations

## REFERENCES

- [1] K. R. Cramer, S. I. Pai, Magneto Fluid Dynamics for Engineers and Applied Physicists, McGraw-Hill Book Co. (1973) New York.
- [2] V. C. A. Ferraro, C. Plumpton, An Introduction to Magneto Fluid Mechanics, Clarendon Press, (1996) Oxford.
- [3] J.A. Shercliff, A Text Book of Magneto Hydrodynamics, Pergamon Press Ltd. (1965) New York.
- [4] G. S. Seth, R. N. Jana, Unsteady hydromagnetic flow in a rotating channel with oscillating pressure gradient, Acta Mechanica, 37 (1980) 29-41.
- [5] G. S. Seth, R. N. Jana, M. K. Maiti, Unsteady hydromagnetic Couette flow in a rotating system, Int. J. Engng. Sci. 20 (1982) 989-999.
- [6] M. Guria, B. K. Das, R. N. Jana, Unsteady hydromagnetic flow in a rotating channel in the presence of inclined magnetic field, Int. J. of Pure and Appl. Math. 32(3) (2006) 379-392.
- [7] V. Vidyandhu, S. D. Nigam, Secondary flow in a rotating channel, J. Math. And Phys. Sci. 1, (1967) 85.
- [8] A. S. Gupta, Magnetohydrodynamic Ekman layer, Acta Mech. 13 (1972) 155.
- [9] R. N. Jana, N. Datta, Couette flow and heat transfer in a rotating system, Acta Mech. 26 (1977) 301.
- [10] B. S. Mazumder, An exact solution of oscillatory Couette flow in a rotating system, ASME J. Appl. Mech. 58 (1991) 1104-1107.
- [11] R. Ganapathy, A note on oscillatory Couette flow in a rotating system, ASME J. Appl. Mech. 61 (1994) 208-209.
- [12] K. D. Singh, An oscillatory hydromagnetic Couette flow with transpiration cooling, Z. Angew. Math. Mech. (ZAMM) 80 (2000) 429-432.

- [13] K. D. Singh, Exact solution of MHD mixed convection periodic flow in a rotating vertical channel with heat radiation. *Int. J. Physical and Mathematical Sciences* 3 (2012) 14-30.
- [14] A. R. Bestman, S. K. Adiepong, Unsteady hydromagnetic free convection flow with radiative heat transfer in a rotating fluid, *Astrophysics and Space Science* 143 (1988)73-80.
- [15] G. S. Seth, R. Nandkeolyar, Md. S. Ansari, Unsteady MHD convective flow within a parallel plate rotating channel with thermal source/sink in a porous medium under slip boundary conditions, *Int. J. of Engng., Sci. and Tech.* 11 (2010) 1-16.
- [16] P. Chandran, N. C. Sacheti, A. K. Singh, Effect of rotation on unsteady hydromagnetic Couette flow, *Astrophys. Space sci.* 202 (1993) 1-10.
- [17] A. K. Singh, N. C. Sacheti, P. Chandran, Transient effects on magnetohydrodynamic Couette flow with rotation: Accelerated motion, *Int. J. Engng. Sci.* 32 (1994) 133-139.
- [18] D. R. V. Prasad Rao, D. V. Krishna, L. Debnath, Combined effect of free and forced convection on MHD flow in a rotating porous channel, *Int. J. Math. and Math. Sci.* 5 (1982) 165-182.
- [19] V. M. Soundalgekar, I. Pop, On hydromagnetic flow in a rotating fluid past an infinite porous plate, *Z. Angew. Math. Mech. (ZAMM)* 53 (1973) 718.
- [20] K. D. Singh, A. Mathew, Injection/suction effect on an oscillatory hydromagnetic flow in rotating horizontal porous channel, *Indian J. Phys.* 82 (2008) 435-445.
- [21] K. D. Alagoa, G. Tay, T. M. Abbey, Radiative and free convective effects of a MHD flow through a porous medium between infinite parallel plates with time-dependent suction, *Astrophysics and Space Science* 260 (1999) 455-468.
- [22] P. Mebine, Radiation effects on MHD Couette flow with heat transfer between two parallel plates, *Global J Pure Appl. Math.* 3 (2007) 191-202.
- [23] K. D. Singh, Rakesh Kumar, Radiation effects on the exact solution of free convective oscillatory flow through porous medium in a rotating vertical channel, *J. of Rajasthan Acad. Phy. Sci.* 8(3) (2009) 295-310.
- [24] K. D. Singh, B. P. Garg, Exact solution of an oscillatory free convective MHD flow in a rotating porous channel with radiative heat, *Proc. Nat. Acad. Sci. India* 80 (2010) 81-89.
- [25] B. P. Garg, Combined effects of thermal radiations and Hall current on moving vertical porous plate in a rotating system with variable temperature, *International Journal of Pure & Applied Mathematics* 81(2) (2012) 335-345.
- [26] K. D. Singh, Oscillatory MHD convective flow of a viscoelastic fluid through a porous medium in a rotating vertical channel in slip-flow regime with thermal radiation and Hall current, *J. of Energy, Heat and Mass Transfer* 35 (2013) 109-132.
- [27] K. D. Singh, R. Kumar, Fluctuating heat and mass transfer on unsteady MHD free convection flow of radiating and reacting fluid past a vertical porous plate in slip-flow regime, *Journal of Applied Fluid Mechanics* 4 (2011) 101-106.
- [28] R. Kumar, K. D. Singh, Mathematical modeling of solet and Hall effects on oscillatory MHD free convective flow of radiating fluid in a rotating vertical porous channel filled with porous medium, *Int. J. of Appl. Math. Mech.* 8 (2012) 49-68.
- [29] K. D. Singh, Khem Chand, Shavnam Sharma, Heat and Mass transfer in an unsteady MHD free convective flow through a porous medium bounded by vertical porous channel in the presence of radiative heat and Hall current, *Int. J. Math. Sci. & Engng. Appl.* 6 (2012) 317-336.
- [30] B. P. Garg, Magnetohydrodynamics and radiation effects on the flow due to moving vertical porous plate with variable temperature, *Proc. Nat. Acad. Sci.* 83 (4), (2013) 327-331.
- [31] B. D. Coleman, W. Noll, An approximation theorem for functional, with applications in continuum mechanics, *Archive for Rational Mechanics and Analysis* 6 (1960) 355-370.
- [32] H. Markovitz, B. D. Coleman, Incompressible second order fluids, *Advances in Applied Mechanics*, 8 (1964) 69-101.

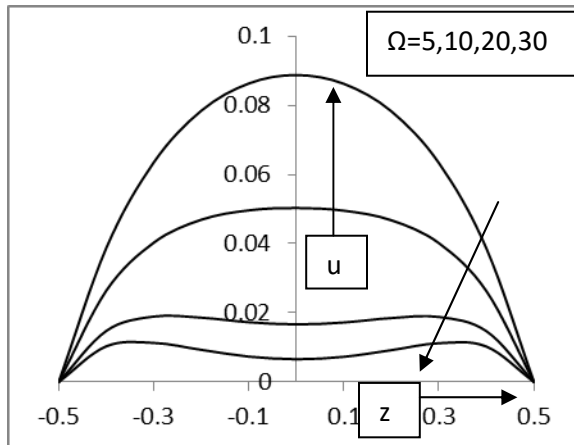


Figure 2. Velocity variation with rotation parameter  $\Omega$  for  $t=0$ .

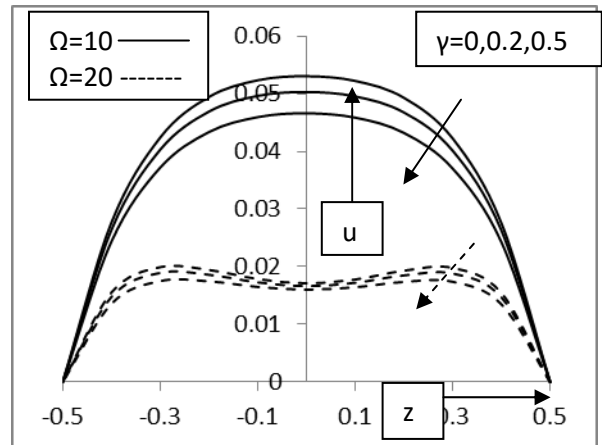


Figure 3. Velocity variation with viscoelastic parameter  $\gamma$  for  $t=0$ .

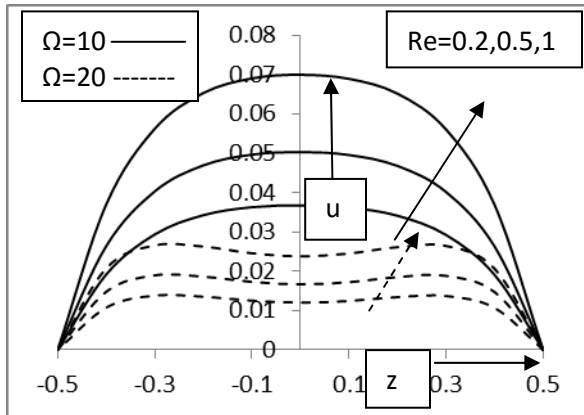


Figure 4. Velocity variation with Reynolds number Re for  $t=0$ .

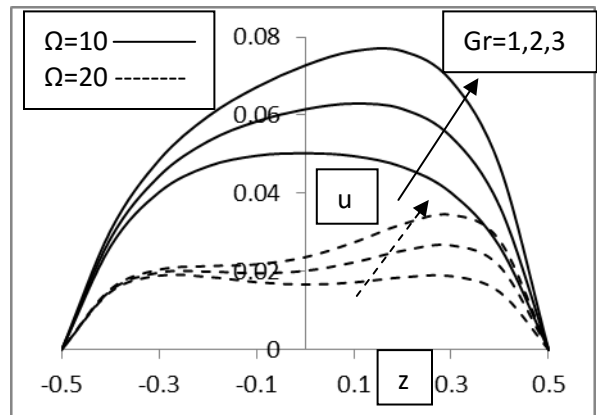


Figure 5. Velocity variation with Grashof number Gr for  $t=0$ .

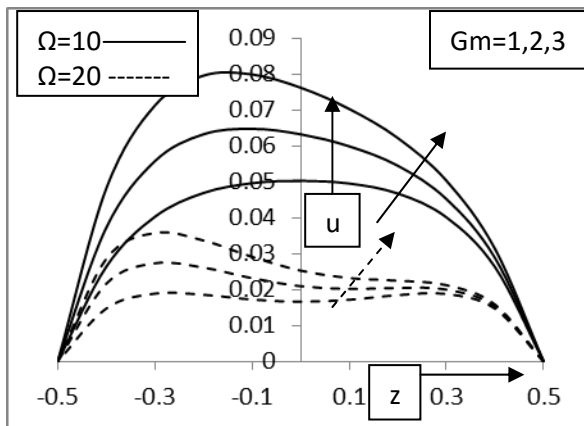


Figure 6. Velocity variation with modified Grashof number Gm for  $t=0$ .

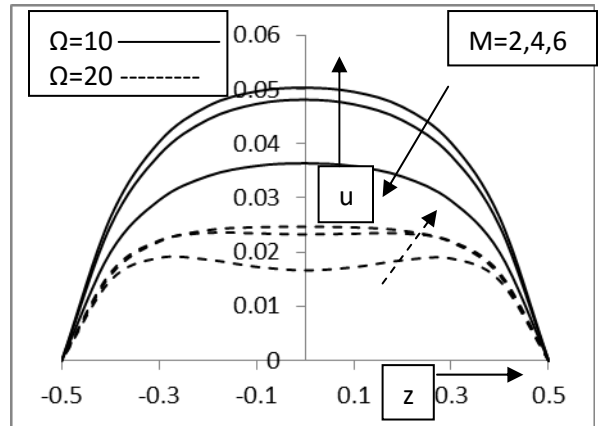


Figure 7. Velocity variation with Hartmann number M for  $t=0$ .

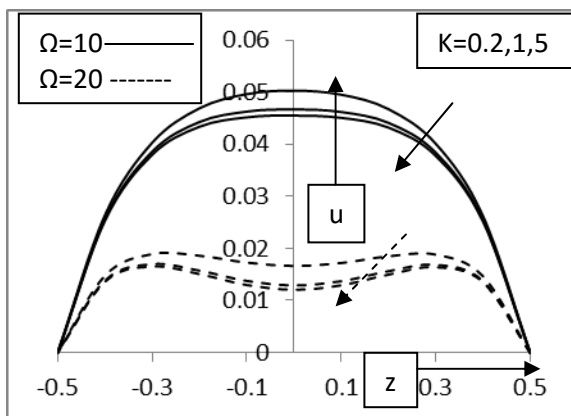


Figure 8. Velocity variation with permeability parameter K for  $t=0$ .

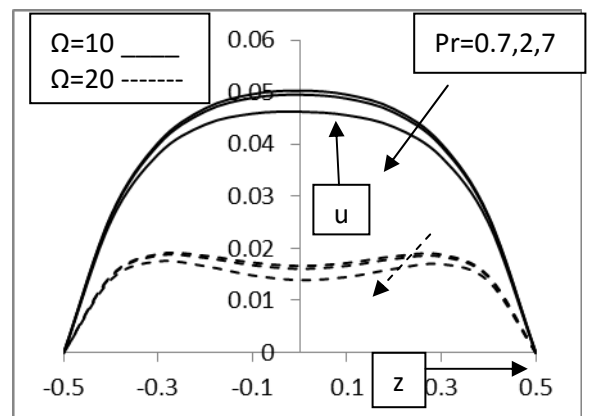


Figure 9. Velocity variation with Prandtl number Pr for  $t=0$ .

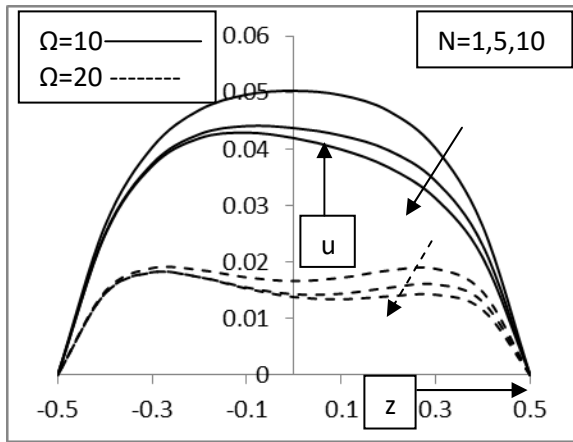


Figure 10. Velocity variation with radiation parameter  $N$  for  $t=0$ .

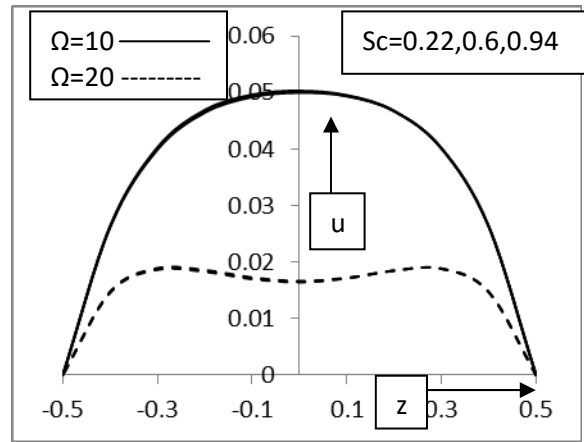


Figure 11. Velocity variation with Schmidt number  $S_c$  for  $t=0$ .

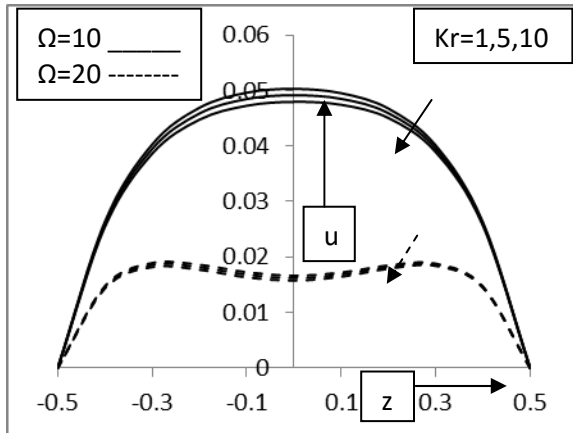


Figure 12. Velocity variation with reaction parameter  $K_r$  for  $t=0$ .

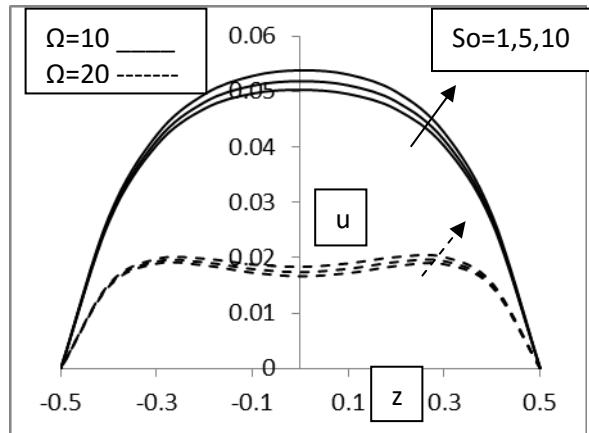


Figure 13. Velocity variation with sores parameter  $S_o$  for  $t=0$ .

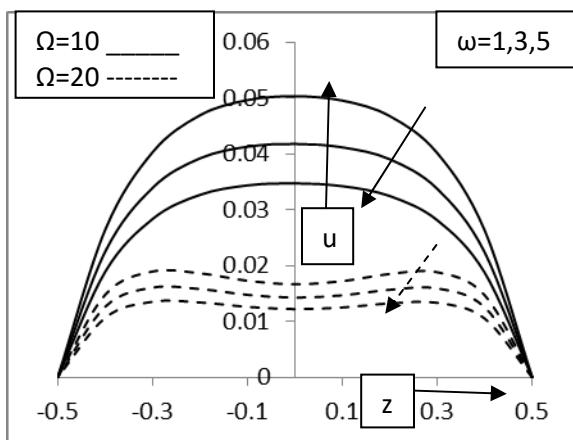


Figure 13. Velocity variation with oscillations  $\omega$  for  $t=0$ .

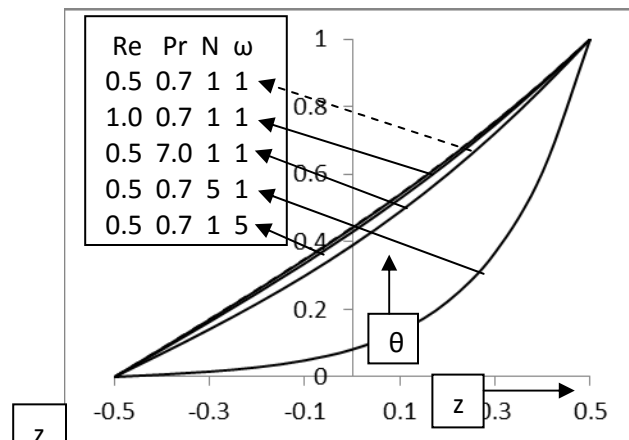


Figure 14. Temperature variation for  $t=0$ .

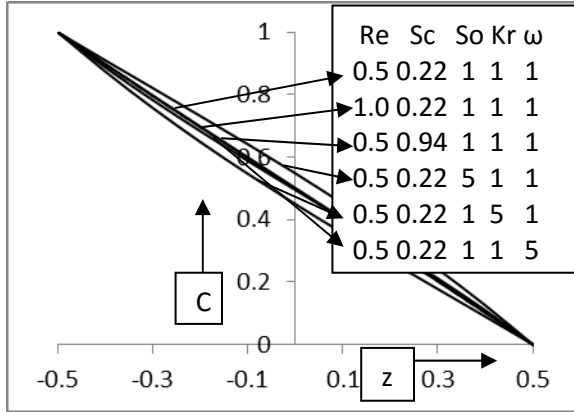


Figure 15. Variation of species concentration for  $t=0$ .

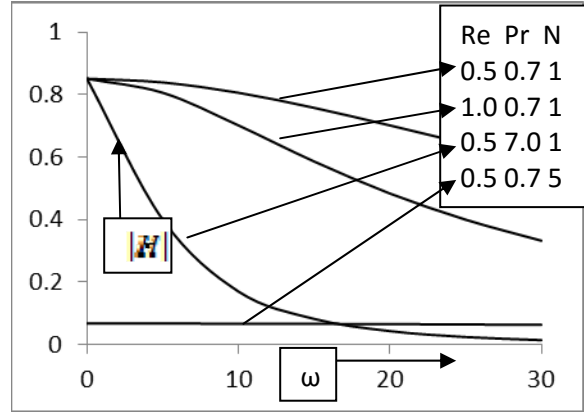


Figure 16. Amplitude of Nusselt number.

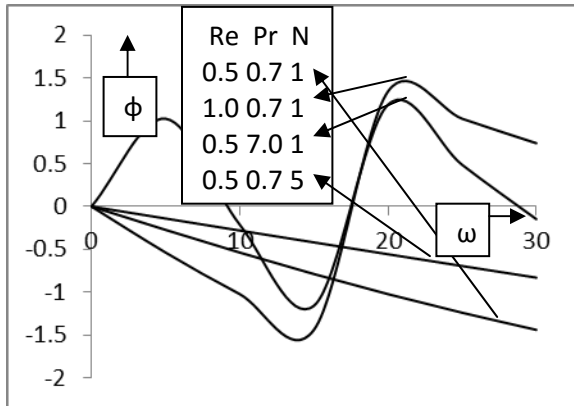


Figure 17. Phase angle of Nusselt number.

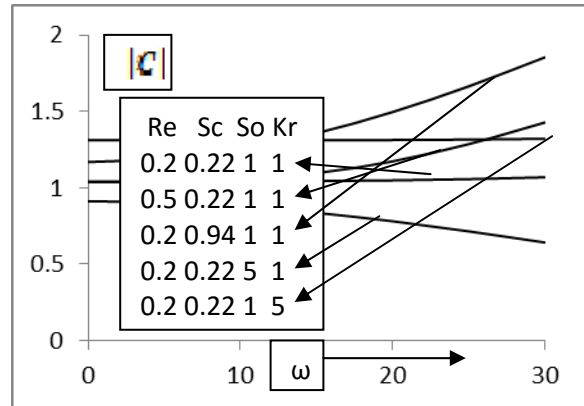


Figure 18. Amplitude of Sherwood number.

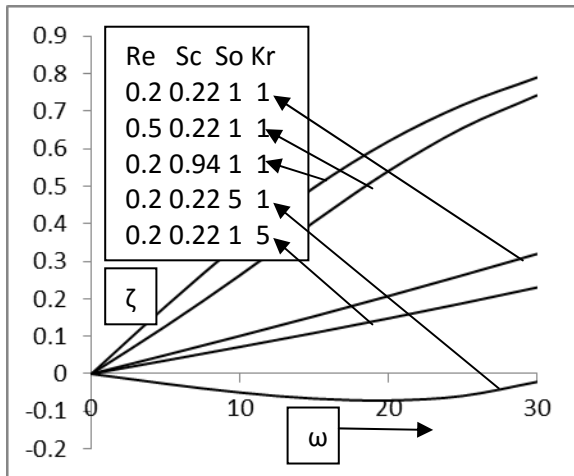


Figure 20. Phase angle of Sherwood number.

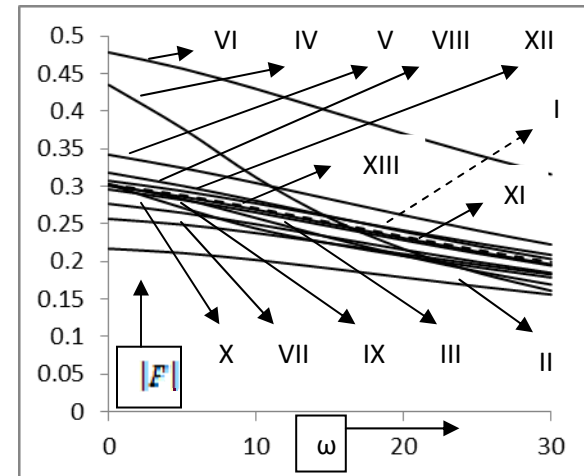


Figure 29. Amplitude of skin friction.

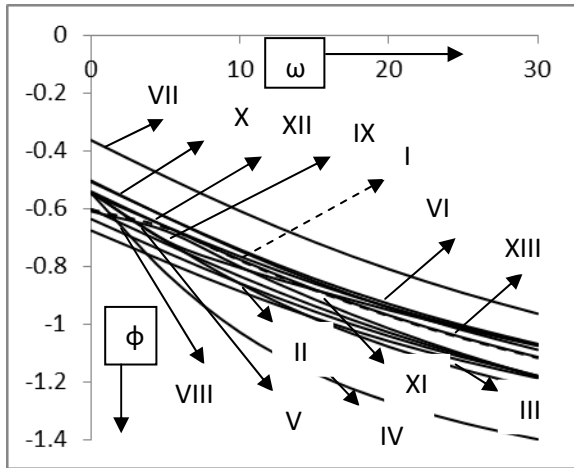


Figure 22. Phase angle of skin friction.

Table 1. Sets of parameters plotted in Figs. 21 & 22.

$\Omega$	$\gamma$	Re	Gr	Gm	M	K	Pr	N	Sc	So	Kr	Curves
10	0.2	0.2	1	1	2	0.2	0.7	1	0.22	1	1	I (---)
20	0.2	0.2	1	1	2	0.2	0.7	1	0.22	1	1	II
10	0.3	0.2	1	1	2	0.2	0.7	1	0.22	1	1	III
10	0.2	0.5	1	1	2	0.2	0.7	1	0.22	1	1	IV
10	0.2	0.2	2	1	2	0.2	0.7	1	0.22	1	1	V
10	0.2	0.2	1	2	2	0.2	0.7	1	0.22	1	1	VI
10	0.2	0.2	1	1	4	0.2	0.7	1	0.22	1	1	VII
10	0.2	0.2	1	1	2	1.0	0.7	1	0.22	1	1	VIII
10	0.2	0.2	1	1	2	0.2	7.0	1	0.22	1	1	IX
10	0.2	0.2	1	1	2	0.2	0.7	5	0.22	1	1	X
10	0.2	0.2	1	1	2	0.2	0.7	1	0.94	1	1	XI
10	0.2	0.2	1	1	2	0.2	0.7	1	0.22	5	1	XII
10	0.2	0.2	1	1	2	0.2	0.7	1	0.22	1	5	XIII